Testing Deconfinement at High Isospin Density

M. Di Toro[1], A. Drago[2], T. Gaitanos[3], V. Greco[1], A. Lavagno[4]

[1] *Università di Catania and INFN, Lab. Nazionali del Sud, 95123 Catania, Italy*

[2] *Dip. di Fisica, Univ. Ferrara and INFN, Sez. Ferrara, 44100 Ferrara, Italy*

[3] *Dept. für Physik, Universität München, D-85748 Garching, Germany*

[4] *Dip. di Fisica, Politecnico di Torino*

E-mail: ditoro@lns.infn.it

Abstract

We study the transition from hadronic matter to a mixed phase of quarks and hadrons at high baryon and isospin densities reached in heavy ion collisions. We focus our attention on the role played by the nucleon symmetry energy at high density.In this respect the inclusion of a scalar isovector meson, the δ-coupling, in the Hadron Lagrangian appears rather important. We study in detail the formation of a drop of quark matter in the mixed phase, and we discuss the effects on the quark drop nucleation probability of the finite size and finite time duration of the high density region. We find that, if the parameters of quark models are fixed so that the existence of quark stars is allowed, then the density at which a mixed phase starts forming drops dramatically in the range $Z/A \sim 0.3$–0.4. This opens the possibility to verify the Witten-Bodmer hypothesis on absolute stability of quark matter using ground-based experiments in which neutron-rich nuclei are employed. These experiments can also provide rather stringent constraints on the Equation of State (EoS) to be used for describing the pre-Supernova gravitational collapse. Consistent simulations of neutron rich heavy ion collisions are performed in order to show that even at relatively low energies, in the few $AGeV$ range, the system can enter such unstable mixed phase. Some precursor observables are suggested, in particular a "neutron trapping" effect.

Key words: Deconfinement at high baryon density, Asymmetric Nuclear Matter, Relativistic Heavy Ion Collisions, Quark Stars
PACS: 25.70.-q,25.75.-q,24.85.+p,21.65.+f,26.60.+c

1 Introduction

Hadronic matter is expected to undergo a phase transition into a deconfined phase of quarks and gluons at large densities and/or high temperatures. On

very general grounds, the transition's critical densities are expected to depend on the isospin of the system, but no experimental test of this dependence has been discussed in the literature. Up to now, experimental data on the phase transition have been extracted from ultrarelativistic collisions of almost isospin-symmetric nuclei, having a proton fraction $Z/A \sim 0.4$–0.5. Moreover, in those experiments large temperatures are obtained, but the maximum density is not much larger than nuclear matter saturation density ρ_0. Experiments with lower beam energies, in which high baryon densities can be reached, have not been extensively studied with the aim of detecting specific signatures of the transition. The analysis of observations of neutron stars, which are composed of β-stable matter for which $Z/A \lesssim 0.1$, can also provide hints on the structure of extremely asymmetric matter at high density. No data on the quark deconfinement transition is at the moment available for intermediate values of Z/A. Recently it has been proposed by several groups to produce unstable neutron-rich beams at intermediate energies. As we will show, these new experiments open the possibility to explore in laboratory the isospin dependence of the critical densities.

The information coming from experiments with relativistic heavy ions is that, for symmetric or nearly symmetric nuclear matter, the critical density appears to be considerably larger than ρ_0. Concerning non-symmetric matter, general arguments based on Pauli principle suggest that the critical density decreases with Z/A. We want to study in particular the range $Z/A \sim 0.3$–0.4, which can be partially explored using beams of neutron rich nuclei as ^{238}U and more extensively tested in radioactive nuclear beam facilities. This region is also relevant for supernova explosion. Here and in the following we are mainly interested in the transition density separating pure hadronic matter from a mixed phase of hadrons and quarks. The second transition density, separating the mixed phase from the pure quark matter phase, cannot be reached in intermediate energy experiments.

A study of the isospin dependence of the transition densities has been performed up to now, to our knowledge, only by Mueller [1], although in that work only one set of model parameter values is explored. The conclusion of [1] is that, moving from symmetric nuclei to nuclei having $Z/A \sim 0.3$, the critical density is reduced by roughly 10%. In this paper we explore in a more systematic way the model parameters and we estimate the possibility of forming a mixed-phase of quarks and hadrons in experiments at energies of the order of a few GeV per nucleon. Moreover, as a crucial technical refinement of previous analysis, we will discuss in detail the formation of a drop of quark matter, taking into account possible retardation effects associated with a non-vanishing surface tension at the quark-hadron interface. Clearly, since the high density region has a finite size and a finite duration, an "effective" critical (transition) density has to be reached, so that the quark drop nucleation rate is not too small. We show that quark clusters can indeed be produced on the expected

time scale, at a density not much larger than the normal spinodal critical density. The effect of a finite temperature is also taken into account.

Concerning the hadronic phase, we have first used the relativistic non-linear Walecka-type model of Glendenning-Moszkowski ($GM1$, $GM2$, $GM3$) [2]. This effective field Lagrangian is very similar to the one of Ref. [1], but with a different choice of the coupling constants in order to reproduce a softer EoS for symmetric matter at high baryon density. This is in fact more in agreement with relativistic Heavy-Ion-Collision (HIC) data [3,4] and with correlated Dirac-Brueckner-Hartree-Fock ($DBHF$) [5,6,7,8] results, see the discussion in Refs. [9,10,11]. The isovector part is treated analogously to the isoscalar part, by introducing a coupling to a vector charged meson. To further explore the sensitivity of our results on the hadronic EoS, a large part of our work is devoted to investigating the possibility of enhancing the symmetry repulsion at high baryon density by introducing a coupling to a charged scalar δ-meson. As remarked in Ref.[12], this is fully in agreement with the spirit of effective field theories, and of course with the phenomenology of the free nucleon-nucleon interaction.

For the quark phase we have considered the MIT bag model [13] at first order in the strong coupling constant α_s [14,1]. In order to show the soundness of the discussed effects, in some cases we have repeated the calculations also using the Color Dielectric Model (CDM) [15,16,17] for the quark phase. In the latter, quarks develop a density dependent constituent mass through their interaction with a scalar field representing a multi-gluon state. In particular we will be interested in those parameter sets which would allow the existence of quark stars [18,19,20], i.e. parameters sets for which the so-called Witten-Bodmer hypothesis is satisfied [21,22]. According to that hypothesis, a state made of an approximately equal number of up, down and strange quarks can have an energy per baryon number E/A smaller than that of iron ($E_{Fe} \approx 930 \ MeV$). To satisfy the Witten-Bodmer hypothesis, strong constraints on quark model parameters have to be imposed. For instance, using the basic version of the MIT bag model, the so-called pressure-of-the-vacuum parameter B must have a very small value, $B^{1/4} \sim 140$–$150 \ MeV$ [14,20]. Taking into account the possibility of forming a diquark condensate, quark stars can exist also for larger values of the pressure of the vacuum, up to $B^{1/4} \sim 160$–$180 \ MeV$ [23,24], depending on the type and size of the superconducting gap. These are the largest values of B that we will discuss in our analysis, since one of the aim of our paper it to show that if quark stars are indeed possible, it is then very likely to find signals of the formation of a mixed quark-hadron phase in intermediate-energy heavy-ion experiments. Assuming Witten-Bodmer hypothesis to be true, ordinary nuclear matter would be metastable. In order not to contradict the obvious stability of normal nuclei, quark matter made of only two flavors must not be more stable than iron. Slightly more strict boundaries on parameters' value can be imposed by requiring not only iron,

but also neutron rich nuclei like e.g. lead, to be stable. If the Witten-Bodmer hypothesis is satisfied, self-bound stars entirely composed of quark matter can exist [18,19,20]. Recently several analysis of observational data have emphasized the possible existence of compact stars having very small radii, of the order of 9 kilometers or less [25,26,27,28]. The most widely discussed possibility to explain the observed mass-radius relation is based on the existence of quark stars. It is therefore particularly interesting to envisage laboratory experiments testing the possible signatures of model parameters values that would allow the existence of these extremely compact stellar objects. What we are proposing in this paper is to use beams of neutron-rich nuclei to this purpose.

It is rather unlikely, at least in the near future, that neutron rich nuclei obtainable in radioactive beam facilities can be accelerated to very large energies, much larger than a few GeV per nucleon. On the other hand, these energies are sufficient to our purposes. The scenario we would like to explore corresponds to the situation realized in experiments at moderate energy, in which the temperature of the system is at maximum of the order of a few ten MeV. In this situation, only a tiny amount of strangeness can be produced and therefore in this paper we only study the deconfinement transition from nucleonic matter into up and down quark matter.

After having chosen a model for the hadronic and for the quark EoS, the deconfinement phase transition is then described by imposing Gibbs equilibrium conditions [29,30].

In order to check if the mixed phase region can be reached in realistic heavy ion collisions at relativistic energies we have performed "ab initio" reaction simulations using relativistic transport equations. With the same effective lagrangians discussed above we have analyzed collisions of neutron rich nuclei, as $^{132}Sn +^{132}Sn$ and the less exotic $^{238}U +^{238}U$, at 1 $AGeV$ beam energies. Since at this low energy the interacting system enters only marginally the mixed phase, we have devoted a whole section to discuss the nucleation mechanism for quark cluster formation, typical of the metastable regions. We show that quark clusters can be produced with this mechanism even on a short time-scale, of the order of $\simeq 10fm/c$, expected for the lifetime of a transient state of very exotic interaction matter formed during the reaction dynamics.

Due to the different relevance of the symmetry repulsion in the hadronic and quark phases we observe a clear "neutron distillation" to the quark clusters (*neutron trapping* effect), in particular just above the transition density. This suggests a series of possible observables rather sensitive to the deconfinement transition at high baryon density.

2 Equations of State

Hadronic Matter

A Relativistic Mean Field (RMF) approach to nuclear matter with the coupling to an isovector scalar field, a virtual $a_0(980)$ δ-meson, has been studied for asymmetric nuclear matter at low densities, including its linear response [31,12,32], and for heavy ion collisions at intermediate energies, where larger density and momentum regions can be probed, [9,10,11]. In this work we extend the analysis of the contribution of the δ-field in dense asymmetric matter to the transition to a deconfined phase.

A Lagrangian density of the interacting many-particle system consisting of nucleons, isoscalar (scalar σ, vector ω), and isovector (scalar δ, vector ρ) mesons is the starting point of our RMF approach. We will call this the $Non-Linear(\rho, \delta)$ model, $NL\rho$ and $NL\rho\delta$:

$$
\begin{aligned}
\mathcal{L} = &\ \bar{\psi}[i\gamma_\mu \partial^\mu - (M - g_\sigma \phi - g_\delta \vec{\tau} \cdot \vec{\delta}) - g_\omega \gamma_\mu \omega^\mu - g_\rho \gamma^\mu \vec{\tau} \cdot \vec{b}_\mu]\psi \\
&+ \frac{1}{2}(\partial_\mu \phi \partial^\mu \phi - m_\sigma^2 \phi^2) - U(\phi) + \frac{1}{2}m_\omega^2 \omega_\mu \omega^\mu + \frac{1}{2}m_\rho^2 \vec{b}_\mu \cdot \vec{b}^\mu \\
&+ \frac{1}{2}(\partial_\mu \vec{\delta} \cdot \partial^\mu \vec{\delta} - m_\delta^2 \vec{\delta^2}) - \frac{1}{4}F_{\mu\nu}F^{\mu\nu} - \frac{1}{4}\vec{G}_{\mu\nu}\vec{G}^{\mu\nu},
\end{aligned} \tag{1}
$$

where (ϕ, ω_μ) are the isoscalar (scalar, vector) meson fields, while the ($\vec{\delta}$, $\vec{b}_\mu$) are the corresponding isovector ones. $F_{\mu\nu} \equiv \partial_\mu \omega_\nu - \partial_\nu \omega_\mu$, $\vec{G}_{\mu\nu} \equiv \partial_\mu \vec{b}_\nu - \partial_\nu \vec{b}_\mu$, and the $U(\phi)$ is a nonlinear potential of σ meson : $U(\phi) = \frac{1}{3}a\phi^3 + \frac{1}{4}b\phi^4$. We remind that the Glendenning-Moszkowski ($GM1$, $GM2$, $GM3$) [2] Lagrangians have exactly the same form, but for the δ-field contribution.

The field equations in RMF approximation are

$$
\begin{aligned}
&(i\gamma_\mu \partial^\mu - (M - g_\sigma \phi - g_\delta \tau_3 \delta_3) - g_\omega \gamma^0 \omega_0 - g_\rho \gamma^0 \tau_3 b_0)\psi = 0, \\
&m_\sigma^2 \phi + a\phi^2 + b\phi^3 = g_\sigma <\bar{\psi}\psi> = g_\sigma \rho_s, \\
&m_\omega^2 \omega_0 = g_\omega <\bar{\psi}\gamma^0 \psi> = g_\omega \rho, \\
&m_\rho^2 b_0 = g_\rho <\bar{\psi}\gamma^0 \tau_3 \psi> = g_\rho \rho_3, \\
&m_\delta^2 \delta_3 = g_\delta <\bar{\psi}\tau_3 \psi> = g_\delta \rho_{s3},
\end{aligned} \tag{2}
$$

where $\rho_3 = \rho_p - \rho_n$ and $\rho_{s3} = \rho_{sp} - \rho_{sn}$, ρ and ρ_s are the baryon and the scalar densities, respectively.

Neglecting the derivatives of mesons fields, the energy-momentum tensor is given by

$$T_{\mu\nu} = i\bar{\psi}\gamma_\mu\partial_\nu\psi + [\frac{1}{2}m_\sigma^2\phi^2 + U(\phi) + \frac{1}{2}m_\delta^2\vec{\delta}^2 - \frac{1}{2}m_\omega^2\omega_\lambda\omega^\lambda - \frac{1}{2}m_\rho^2\vec{b_\lambda}\vec{b^\lambda}]g_{\mu\nu}. \quad (3)$$

The EoS for nuclear matter with the isovector scalar field at finite temperature in RMF is given by the energy density

$$\epsilon = 2\sum_{i=n,p}\int\frac{\mathrm{d}^3k}{(2\pi)^3}E_i^*(k)(n_i(k) + \bar{n}_i(k)) + \frac{1}{2}m_\sigma^2\phi^2$$
$$+U(\phi) + \frac{1}{2}m_\omega^2\omega_0^2 + \frac{1}{2}m_\rho^2b_0^2 + \frac{1}{2}m_\delta^2\delta_3^2 \ , \quad (4)$$

and pressure

$$P = \frac{2}{3}\sum_{i=n,p}\int\frac{\mathrm{d}^3k}{(2\pi)^3}\frac{k^2}{E_i^*(k)}(n_i(k) + \bar{n}_i(k)) - \frac{1}{2}m_\sigma^2\phi^2$$
$$-U(\phi) + \frac{1}{2}m_\omega^2\omega_0^2 + \frac{1}{2}m_\rho^2b_0^2 - \frac{1}{2}m_\delta^2\delta_3^2 \ , \quad (5)$$

where $E_i^* = \sqrt{k^2 + m_i^{*2}}$. The nucleon effective masses are defined as

$$m_i^* = M - g_\sigma\phi \mp g_\delta\delta_3 \quad (- \ proton, + \ neutron). \quad (6)$$

The $n_i(k)$ and $\bar{n}_i(k)$ are the fermion and antifermion distribution functions for protons $(i = p)$ and neutrons $(i = n)$:

$$n_i(k) = \frac{1}{1 + \exp\{(E_i^*(k) - \mu_i^*)/T\}} \ , \quad (7)$$

and

$$\bar{n}_i(k) = \frac{1}{1 + \exp\{(E_i^*(k) + \mu_i^*)/T\}}. \quad (8)$$

where the effective chemical potential μ_i^* is determined by the nucleon density

$$\rho_i = 2\int\frac{\mathrm{d}^3k}{(2\pi)^3}(n_i(k) - \bar{n}_i(k)) \ , \quad (9)$$

and the μ_i^* is related to the chemical potential μ_i in terms of the vector meson mean fields by the equation

$$\mu_i^* = \mu_i - g_\omega \omega_0 \mp g_\rho b_0 \quad (- \; proton, + \; neutron), \tag{10}$$

where μ_i are the thermodynamical chemical potentials $\mu_i = \partial\epsilon/\partial\rho_i$. At zero temperature they reduce to the Fermi energies $E_{Fi} \equiv \sqrt{k_{Fi}^2 + m_i^{*2}}$.

The proton and neutron chemical potentials can be written in terms of the baryon and isospin chemical potentials by the equations

$$\mu_p = \mu_B + \mu_3, \qquad \mu_n = \mu_B - \mu_3. \tag{11}$$

The scalar density ρ_s is given by

$$\rho_s = 2 \sum_{i=n,p} \int \frac{d^3k}{(2\pi)^3} \frac{m_i^*}{E_i^*} (n_i(k) + \bar{n}_i(k)) . \tag{12}$$

where the Fermi momentum k_{F_i} of the nucleon is related to its density, $k_{F_i} = (3\pi^2 \rho_i)^{1/3}$.

In the presence of a coupling to an isovector-scalar δ-meson field, the expression for the symmetry energy at $T = 0$ has a simple transparent form, see [12,32]:

$$E_{sym}(\rho) = \frac{1}{6} \frac{k_F^2}{E_F} + \frac{1}{2} [f_\rho - f_\delta (\frac{m^*}{E_F^*})^2] \rho , \tag{13}$$

where $m^* = M - g_\sigma \phi$ and $E_F{}^* = \sqrt{k_F^2 + m^{*2}}$. We clearly see the mechanism which is behind the apparent paradox of an attracting contribution of the isovector scalar field leading to a larger repulsion of the symmetry term. In fact, at normal density a larger $\rho - meson$ coupling is needed in order to reproduce the correct symmetry energy coefficient of the Bethe-Weiszäcker mass formula. When the baryon density increases, the δ contribution is quenched by the $(m^*/E_F^*)^2$ factor and we are left with a stiffer symmetry term. The isovector coupling constants, both in the $NL\rho$ and in the $NL\rho\delta$ cases, are fixed from the symmetry energy at saturation and from Dirac-Brueckner estimations, see the detailed discussions in Refs. [12,32].

It is interesting to compare the predictions on the transition to a deconfined phase of the two effective Lagrangians $GM3$ and $NL\rho\delta$. The isoscalar part is very similar in the two models and at high densities it approaches Dirac-Brueckner predictions, as already noted. The isovector part is quite different, because in $GM3$ we only have the coupling to the vector ρ-field, while in $NL\rho\delta$ we also have the contribution of the δ-field, which leads to a stiffer symmetry term and to a neutron/proton effective mass splitting. We remind that recently the latter interaction has been used with success to describe reaction observables in RMF-transport simulations of relativistic heavy ion collisions, where high densities and momenta are reached [9,10,11].

The coupling constants, $f_i \equiv g_i^2/m_i^2$, $i = \sigma, \omega, \rho, \delta$, and the two parameters of the σ self-interacting terms: $A_\sigma \equiv a/g_\sigma^3$ and $B_\sigma \equiv b/g_\sigma^4$ for the two hadron effective interactions are reported in Tab. 1. The corresponding properties of nuclear matter are listed in Tab. 2.

Table 1. Parameter sets.

Parameter	$NL\rho$	$NL\rho\delta$	$GM1$	$GM2$	$GM3$
f_σ (fm^2)	10.329	10.329	11.79	9.148	9.923
f_ω (fm^2)	5.423	5.423	7.149	4.82	4.82
f_ρ (fm^2)	0.95	3.150	1.103	1.198	1.198
f_δ (fm^2)	0.00	2.500	0.00	0.00	0.00
A_σ (fm^{-1})	0.033	0.033	0.014	0.016	0.041
B_σ	-0.0048	-0.0048	-0.001	0.013	-0.0024

Table 2. Saturation properties of nuclear matter.

	$NL\rho, NL\rho\delta$	$GM1$	$GM2$	$GM3$
ρ_0 (fm^{-3})	0.160	0.153	0.153	0.153
E/A (MeV)	-16.0	-16.3	-16.3	-16.3
K (MeV)	240.0	300.0	300.0	240.0
E_{sym} (MeV)	31.3	32.5	32.5	32.5
M^*/M	0.75	0.70	0.78	0.78

Quark Matter

In our calculations we will use both a "minimal" version of the MIT Bag model [13], in which the interaction inside the bag is neglected, and also a model

taking into account corrections at first order in the strong coupling constant α_s [14,1]. We will also display results obtained using the CDM [15,16,17]. We will limit our study to the two-flavor case ($q = u, d$). As already remarked in the introduction, this appears well justified for the application to heavy ion collisions at relativistic (but not ultra-relativistic) energies. The fraction of strangeness produced at these energies is very small [33]. In our analysis we have not taken into account the possibility of forming a diquark condensate. Clearly, the superconducting gaps accessible in the scenario we are discussing are the ones pairing up and down quarks only. Moreover, the gap can be suppressed in the reaction case for several reasons: finite size of the system [34], different values of the up and down chemical potential (particularly so for the strongly asymmetric matter we are discussing in our paper) and finally for the relatively high temperature always reached in the high density stage of a reaction (see Sects.IV and V).

The energy density, the pressure and the number density for the quark q read:

$$\epsilon = 3 \times 2 \sum_{q=u,d} \int \frac{\mathrm{d}^3 k}{(2\pi)^3} \sqrt{k^2 + m_q^2} (n_q + \bar{n}_q) + B \ , \tag{14}$$

$$P = \frac{3 \times 2}{3} \sum_{q=u,d} \int \frac{\mathrm{d}^3 k}{(2\pi)^3} \frac{k^2}{\sqrt{k^2 + m_q^2}} (n_q + \bar{n}_q) - B \ , \tag{15}$$

$$\rho_i = 3 \times 2 \int \frac{\mathrm{d}^3 k}{(2\pi)^3} (n_i - \bar{n}_i) \ , \qquad i = u, d \ ; \tag{16}$$

where B denotes the bag pressure, m_q the quark masses, and $n_q, \bar{n}_q$ indicate the Fermi distribution functions for quarks and antiquarks respectively:

$$n_q = \frac{1}{1 + \exp\{(E_q - \mu_q)/T\}} \ , \tag{17}$$

and

$$\bar{n}_q = \frac{1}{1 + \exp\{(E_q + \mu_q)/T\}} \ . \tag{18}$$

Here $E_q = \sqrt{k^2 + m_q^2}$ and μ_q are the chemical potentials for quarks and antiquarks of type q. The latter are related to the baryon and isospin chemical potential

$$\mu_u = \frac{1}{3}\mu_B + \mu_3 , \qquad \mu_d = \frac{1}{3}\mu_B - \mu_3 . \qquad (19)$$

The quark densities are related to the baryon and isospin densities by the following equations

$$\rho_B = \frac{\rho_u + \rho_d}{3} , \qquad \rho_3 = \rho_u - \rho_d . \qquad (20)$$

We have considered massless u, d quarks and a range of bag constants, between $B = (140 \ MeV)^4$ and $B = (170 \ MeV)^4$. These are smaller values than the one used in Ref.[1], $B = (190 \ MeV)^4$. On the other hand this parameter range covers almost completely the one which can give origin to quark stars, even taking into account the formation of a diquark condensate. As already mentioned, we also present results obtained taking into account corrections at first order in α_s. Explicit formulae for the contribution of the gluon exchange to energy and pressure can be found e.g. in Ref. [35].

No density dependence for the bag pressure has been introduced, but in the CDM, that we have also explored, something similar to a density dependent B exists, namely the contribution of the scalar field mimicking a multi-gluon state. The Lagrangian of the CDM reads:

$$L = i\bar{\psi}\gamma^\mu\partial_\mu\psi + \frac{1}{2}(\partial_\mu\sigma)^2 + \frac{1}{2}(\partial_\mu\vec{\pi})^2 - U(\sigma, \vec{\pi})$$
$$+ \sum_{f=u,d} \frac{g_f}{f_\pi\kappa} \bar{\psi}_f (\sigma + i\gamma_5\vec{\tau}\cdot\vec{\pi}) \psi_f + \frac{1}{2}(\partial_\mu\kappa)^2 - \frac{1}{2}M^2\kappa^2 ,$$

where $U(\sigma, \vec{\pi})$ is the "mexican-hat" potential, as in Ref. [36].

The coupling constants are given by $g_{u,d} = g(f_\pi \pm \xi_3)$, where $f_\pi = 93 \ MeV$ is the pion decay constant and $\xi_3 = f_{K^\pm} - f_{K^0} = -0.75 \ MeV$. These coupling constants depend on a single parameter g. Confinement is obtained via the effective quark masses $m_{u,d} = -g_{u,d}\bar{\sigma}/(\bar{\kappa}f_\pi)$ which diverge outside the nucleon. Working at mean-field level, the only free parameter is actually the product $G = \sqrt{gM}$. In our calculations we have assumed $M=1.7 \ GeV$ and we have explored various values for g. In this model the last term of the lagrangian plays a role similar to the vacuum pressure constant B of the MIT bag model. At variance with the latter, in the CDM the vacuum pressure is density dependent, as anticipated.

Mixed phase

The structure of the mixed phase is obtained by imposing the Gibbs conditions [29,30] for chemical potentials and pressure and by requiring the conservation of the total baryon and isospin densities

$$
\begin{aligned}
\mu_B^{(H)} &= \mu_B^{(Q)} \,, \\
\mu_3^{(H)} &= \mu_3^{(Q)} \,, \\
P^{(H)}(T, \mu_{B,3}^{(H)}) &= P^{(Q)}(T, \mu_{B,3}^{(Q)}) \,, \\
\rho_B &= (1 - \chi)\rho_B^H + \chi\rho_B^Q \,, \\
\rho_3 &= (1 - \chi)\rho_3^H + \chi\rho_3^Q \,,
\end{aligned}
\tag{21}
$$

where χ is the fraction of quark matter in the mixed phase. In this way we get the *binodal* surface which gives the phase coexistence region in the (T, ρ_B, ρ_3) space [30,1]. For a fixed value of the conserved charge ρ_3, related to the proton fraction $Z/A \equiv (1 + \rho_3/\rho_B)/2$, we will study the boundaries of the mixed phase region in the (T, ρ_B) plane. We are particularly interested in the lower baryon density border, i.e. the critical/transition density ρ_{cr}, in order to check the possibility of reaching such (T, ρ_{cr}, ρ_3) conditions in a transient state during a *HIC* at relativistic energies.

In the hadronic phase, if a quadratic form is assumed for the symmetry energy the latter is related to the charge chemical potential by the equation:

$$
\mu_3 = 2E_{sym}(\rho_B)\frac{\rho_3}{\rho_B} \,.
\tag{22}
$$

We expect therefore that our results on the critical density will be rather sensitive to the isovector channel in the hadronic *EoS* at high densities.

3 Results at Zero Temperature

The most plausible way of testing in terrestrial laboratories the possible formation of a mixed phase of hadrons and quarks at high baryon and isospin densities, is via heavy-ion collisions at relativistic energies, as it will be discussed in Secs. IV–VII. It is anyway interesting to investigate the possibility of detecting modifications in the structure of nuclei even with experiments testing densities of the order of ρ_0. This is what is discussed in the present section.
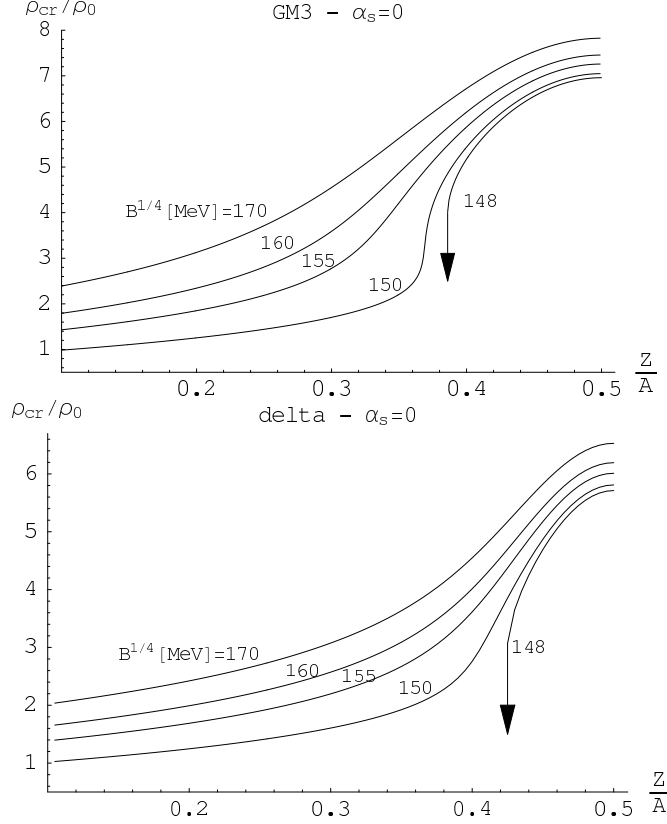
Fig. 1. Transition densities separating hadronic matter from mixed quark-hadron phase at zero temperature. In the upper panel the $GM3$ parametrization has been used for the hadronic EoS, in the lower panel, $NL\rho\delta$ parametrization, see Table 1. The MIT bag model without gluon exchange has been used for the quark EoS. The arrows indicate that the transition density drops to very small values and the parameter $B^{1/4}$ cannot be further reduced.

In Figs. 1, 2, 3 we report the crossing density ρ_{cr} separating nuclear matter from the quark-nucleon mixed phase, as a function of the proton fraction Z/A for various choices of the Hadronic/Quark EoS. Fig. 1 shows the $GM3$ (top panel) vs. $NL\rho\delta$ (bottom panel) coupled to the same no-gluon MIT bag model. We can see the effect of the δ-coupling towards an *earlier* crossing due to the larger symmetry repulsion at high baryon densities. Fig. 2 has been obtained using $GM2$ ($GM1$) parametrization for the hadronic phase and the MIT bag model without gluons (with gluons and $\alpha_s = 0.3$) in the upper and lower window, respectively. Finally in Fig. 3 the same analysis is performed using the CDM for the quark EoS. For values of the parameter g slightly smaller than the one indicated in the figure the critical density drops to a very small value and the situation depicted in Fig.1 using arrows is obtained.

The most striking feature of all results is the sharp decrease of ρ_{cr} in the range $Z/A \sim 0.3$–0.4. The lower curves in each window correspond to parameters' values satisfying Witten-Bodmer hypothesis even in the absence of a diquark condensate. In these cases, and for $Z/A \sim 0.3$, the critical density is of the
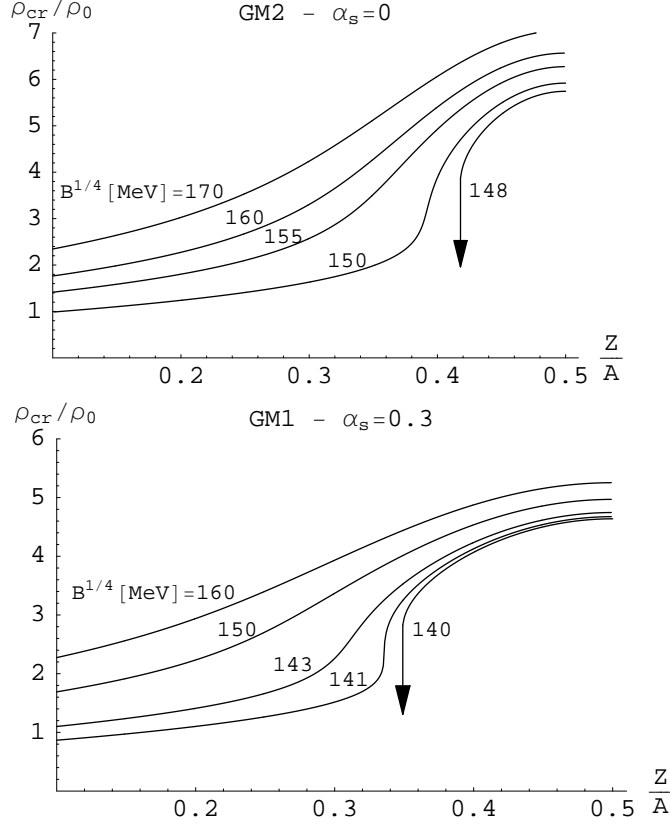
Fig. 2. Similar to Fig.1. In the upper panel the $GM2$ parametrization [2] has been used for the hadronic EoS and the MIT bag model without gluon exchange has been used for the quark EoS. In the lower panel, $GM1$ parametrization [2] for the hadronic EoS and MIT bag model with perturbative exchange of gluons with $\alpha_s = 0.3$.

order of ρ_0. This opens the possibility to test the deconfinement transition even in relatively low energy experiments, possible in future RNB facilities.

The main features can be easily understood if one recalls that we are investigating situations in which the minimum of pure quark matter EoS is at an energy just above or just below the minimum of the hadronic matter EoS. The first scenario is the one in which the absolute minimum of E/A, *for a given value of Z/A*, corresponds to the quark matter EoS (this situation corresponds to very small values of the parameter B, e.g. $B^{1/4} = 148\ MeV$ in Fig. 1). In this case, the deconfinement transition starts at very small densities, even smaller than nuclear matter saturation density. The numerical determination of these densities is rather delicate and we limit ourself to indicate with vertical arrows, like in Fig. 1, the behavior of the crossing density for such value of B. If the value of B is further reduced, the vertical arrow shifts towards larger values of Z/A and therefore cannot correspond to a physically acceptable situation, since it would imply deconfinement into two flavor quark matter at low densities, even for almost symmetric nuclei.
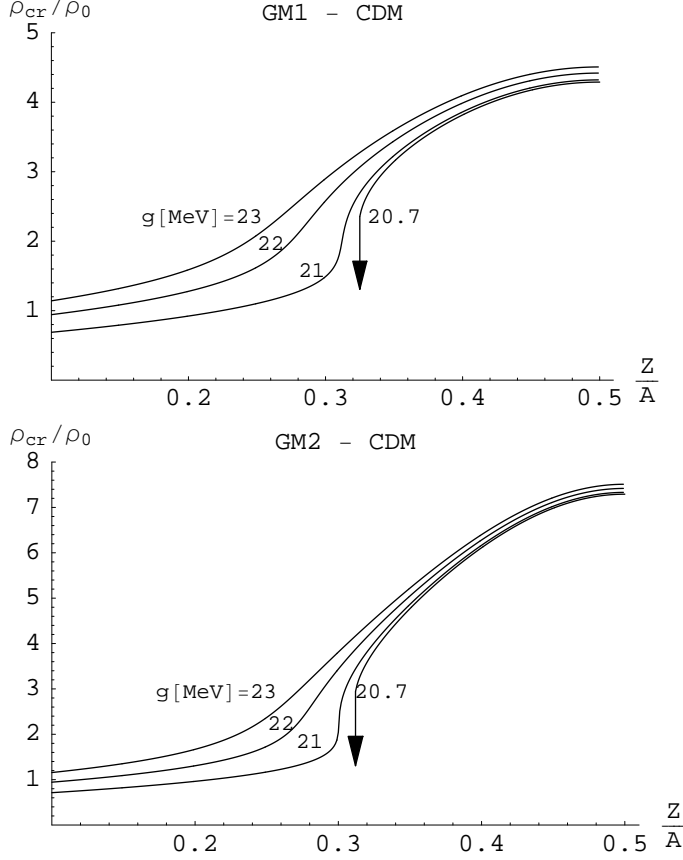
13

Fig. 3. Similar to Fig.1. The quark EoS has been computed using the Color Dielectric Model [17]. The parameter g regulates the coupling between quarks and a scalar multi-gluon field, see text.

The second situation is the one in which the minimum of the quark EoS lies slightly above the hadronic minimum, as e.g. for $B^{1/4} = 150\ MeV$ in the top panel of Fig. 1. In this case the deconfinement transition starts at a density slightly smaller than the one corresponding to the minimum of the quark EoS. The crossing density cannot be further reduced, since at even smaller densities the energy E/A in the quark phase rises dramatically, both in the MIT bag model and in the CDM, and therefore no mixing of hadronic matter with quark matter is possible at those densities.

Finally, when the value of B is further increased, the isospin dependence of the energy becomes percentually smaller, the dependence of the crossing density on the Z/A fraction reduces progressively, and a situation similar to the one discussed in Ref.[1] is reached.

In Fig.4 the effect of the exchange of the charged δ meson is considered in Non-Linear models [12]. The δ-exchange potential provides an extra isospin dependence of the EoS, and its effect shows up in a further reduction of the critical density.
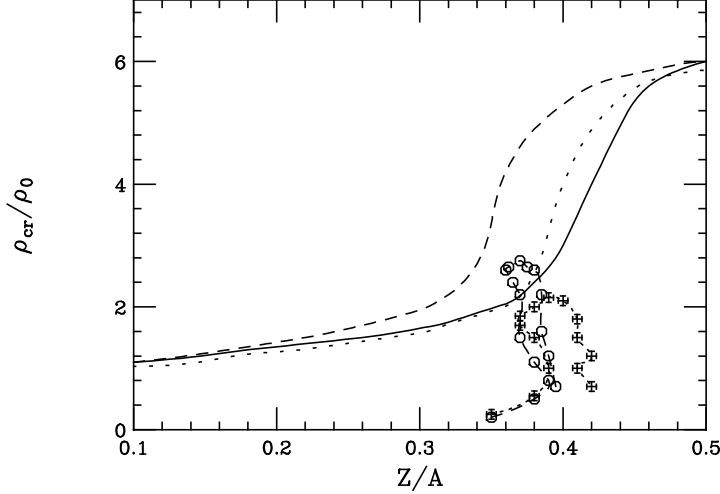
14

Fig. 4. Variation of the transition density with proton fraction for various hadronic *EoS* parameterizations. Dotted line: $GM3$ parametrization [2]; dashed line: $NL\rho$ parametrization [12]; solid line: $NL\rho\delta$ parametrization [12]. For the quark *EoS*, the *MIT* bag model with $B^{1/4}$=150 MeV and α_s=0 has been used. The points represent the path followed in the interaction zone during a semi-central ^{132}Sn+^{132}Sn collision at 1 $AGeV$ (circles) and at 300 $AMeV$ (crosses), see text.

Let us now comment on the physical relevancy of the dramatic reduction of the crossing density in neutron rich nuclei at zero temperature. First, the request that stable neutron-rich nuclei do not dissolve into quarks puts more stringent bounds on the model parameters than the usual request based on iron stability. Second, it is interesting to discuss which could be the signatures of the beginning of the formation of mixed phase, at a density of the order of ρ_0, in neutron rich nuclei. Although we cannot expect to find a direct signal of deconfinement in the structure of these nuclei, we can look for precursor signals. In particular, we expect that the formation of clusters containing six or nine quarks will be enhanced due to the reduction of the crossing deconfinement density. This enhancement can in turn be interpreted as a modification of single-nucleon properties due the nuclear medium. The experimental search of effects like the one we are referring to here has a very long story, which includes the discovery of the *EMC* effect [37]. This is a non trivial difference between free-nucleon and nuclear structure functions, for a review see [38]. In particular models invoking the formation of multi-quark clusters have been rather popular [39,40,41]. Our analysis suggests a dependence of the *EMC* effect on the isospin, since the probability of forming virtual multi-quark bags would be enhanced in neutron rich nuclei. This dependence, which has a many-body origin, would add to non-isoscalarity effects which are in any case present in the different structure functions of neutrons and protons [42]. A full account of in-medium corrections has been attempted in Ref. [43]. A recent attempt at measuring the isospin dependence of the *EMC* effect is reported in Ref.[44].

The above discussed effect around normal density can take place only for
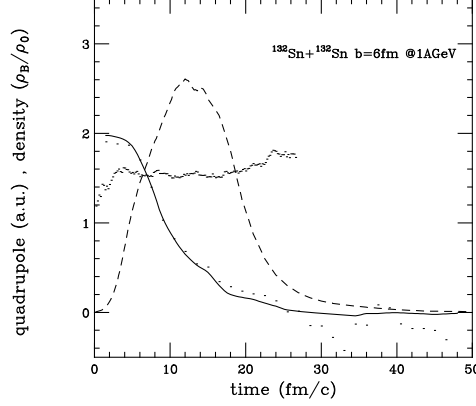
15

Fig. 5. Semicentral $^{132}Sn +^{132} Sn$ collision at 1 $AGeV$. Time evolution of the quadrupole moment in momentum space (solid line) and of the density (dashed line). The simulation examine the after-scattering thermalization inside a cubic cell 2.5 fm wide, located in the center of mass of the system.

rather special values of the model parameters, or for nuclei unrealistically neutron-rich. In the following, therefore, we will discuss effects associated with larger densities, reachable during intermediate-energy heavy ion collisions.

4 Relativistic Transport Simulations: Exotic Transient States

A direct way to explore the reduction of the deconfinement transition density would be to test the EoS of asymmetric matter via collisions of two neutron rich nuclei. This possibility is based on the "ab initio" analysis of intermediate-energy heavy-ion collisions in a Relativistic Mean Field approach, as discussed in Refs.[9,10,11,45,46,33].

^{132}Sn Collisions

We have first performed some simulations of the ^{132}Sn + ^{132}Sn collision (average Z/A=0.38) at various energies, for semicentral impact parameter, b=6 fm, in order to optimize the neutron skin effect and get a large asymmetry in the interaction zone. In order to be fully consistent we have used the same effective interaction $NL\rho\delta$ [12] of the EoS leading to the transition deconfinement density (solid line) of Fig.4. In the same figure we report the paths in the $(\rho, Z/A)$ plane followed in the c.m. region during the collision, at energies of 300 $AMeV$ (crosses) and 1 $AGeV$ (circles). We see that already at 300 $AMeV$ we are reaching the border of the mixed phase, and we are well inside it at 1 $AGeV$. We have also performed another check of feasibility. Since the neutrons in the skin of ^{132}Sn occupy an extended region of very low density, it is
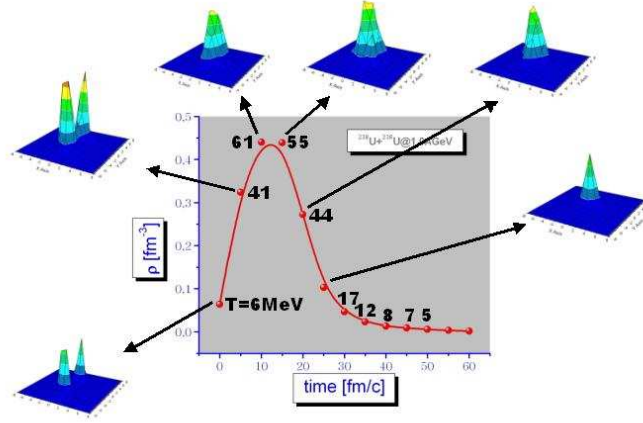
Fig. 6. Uranium-Uranium 1 $AGeV$ semicentral: correlation between density, temperature, momentum thermalization inside a cubic cell 2.5 fm wide, located in the center of mass of the system.

important to check if during the collision the nucleons remain near the c.m. when the center of the system has thermalized. In Fig.5 we show that indeed, when the maximum density is reached ($\rho \sim 2.6\,\rho_0$) the quadrupole moment of the nucleons momentum distribution has dropped to $\sim 10\%$ of its initial value, a signal that the system has indeed thermalized.

The use of an harder hadronic EoS for symmetric matter at high density would correspond to a even more favorable situation than the one presented in Fig.4, as discussed before. Moreover the use of neutron-richer nuclei would allow to test the EoS at smaller values of Z/A. To this purpose, the most promising nuclei are the ones near the r-process path, in particular for neutron numbers near the magic values N=82 or 126. In these regions, the proton fraction is as low as 0.32–0.33 and these nuclei could be studied in future experiments with neutron-rich beams.

^{238}U Collisions

In order to check the possibility of observing some precursor signals of this new physics even in collisions of stable nuclei at intermediate energies we have performed some event simulations for the collision of very heavy, neutron-rich, elements. We have chosen the reaction $^{238}U +^{238} U$ (average proton fraction $Z/A = 0.39$) at 1 $AGeV$ and semicentral impact parameter $b = 7\ fm$ in order to increase the neutron excess in the interacting region. We have used a $NL\rho\delta$ Hadronic Lagrangian in order to optimize the shift of the transition density at high isospin density. We can compare directly the conditions of the nuclear matter at local equilibrium during the reaction evolution with the predictions of the lower panel of Fig.8 obtained with the same interaction. In order to
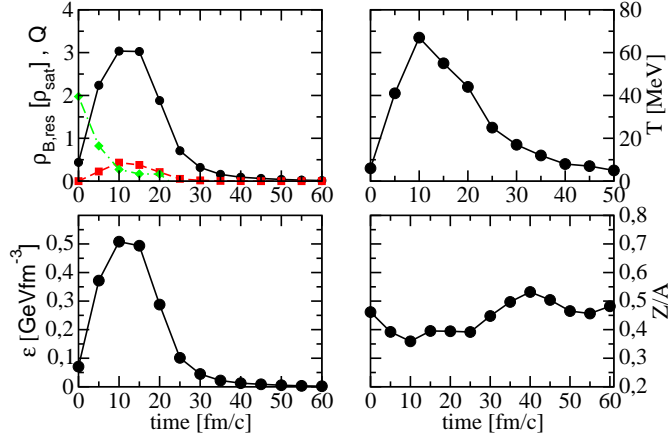
Fig. 7. Uranium-Uranium 1 $AGeV$ semicentral: density, temperature, energy density, momentum, isospin inside a cubic cell 2.5 fm wide, located in the center of mass. Curves in the upper-left panel: *black dots* - baryon density in ρ_0 units; *grey dots* - quadrupole moment in momentum space; *squares* - resonance density.

evaluate the degree of local equilibration and the corresponding temperature we have also followed the momentum distribution in a space cell located in the c.m. of the system, in the same cell we report the maximum mass density evolution. The results are shown in Fig. 6. We see that after about 10 fm/c a nice local equilibration is achieved. We have an unique Fermi distribution and from a simple fit we can derive a local temperature evaluation. At this beam energy the maximum density (about three times ρ_0) coincides with the thermalization at estimated maximum temperatures of $50 - 60$ MeV, then the system is quickly cooling while expanding.

In Fig.7 we report the time evolution of all physics parameters inside the c.m. cell in the interaction region: upper-left panel, baryon and resonance density and quadrupole deformation in momentum space; upper-right panel, local temperature evolution; lower-left panel, energy density; lower-right panel, proton fraction.

We note that a rather exotic nuclear matter is formed in a transient time of the order of 10 fm/c, with baryon density around $3\rho_0$, temperature $50-60$ MeV, energy density 500 MeV fm^{-3} and proton fraction between 0.35 and 0.40, well inside the mixed phase region of the Fig. 8 lower panel, see the next Section.
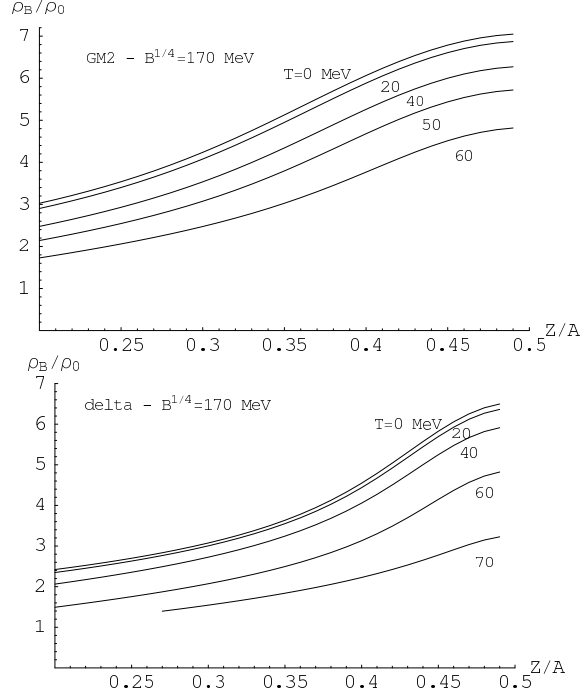
Fig. 8. Transition densities separating hadronic matter from mixed quark-hadron phase at finite temperature. In the upper panel the $GM2$ parametrization has been used for the hadronic EoS, in the lower panel, the $NL\rho\delta$ parametrization. The MIT bag model with $B^{1/4} = 170$ MeV, without gluon exchange, has been used for the quark EoS.
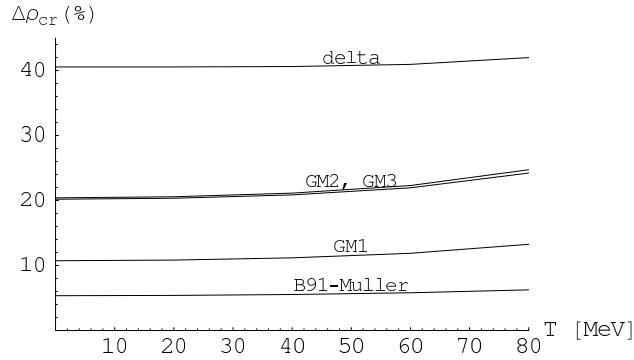

Fig. 9. Percent variation of the transition density at various temperatures, with respect to the symmetric case, for a system with initial proton fraction in the hadronic phase $Z/A = 0.35$. Results are shown for various choices of the hadronic EoS, see text. The quark EoS is the one used by Müller, [1], ($B^{1/4} = 190$ MeV, $\alpha_s = 0.35$).

5   Results at Finite Temperature

As discussed before our aim is finally to suggest possible experiments on heavy ion collisions at intermediate energies. In a realistic collision we cannot have a compression of the interacting system without some heating. This point has been be clearly shown in the Uranium-Uranium results of the previous Section.

Thus, it is essential to extend the previous results to finite temperature cases. The procedure is exactly the same as in the $T = 0$ case, we only have to use the $T \neq 0$ form of the Fermi distributions for nucleons and quarks, Eqs.(7,8) and Eqs.(17,18) respectively.

The thermal motion reduces the critical baryon density for the transition to the mixed phase, in agreement with the results obtained in Ref. [1], although this effect is actually more relevant at higher temperatures, above $T = 60 \ MeV$. Our results are shown in Fig.8 for $GM2$ (upper panel) and $NL\rho\delta$ (lower panel) hadronic EoS. The same quark EoS, the MIT bag model with $B^{1/4} = 170 \ MeV$ and without gluon exchange, has been used in both cases.

We notice again that the larger symmetry repulsion due to the inclusion of the δ-meson is increasing the reduction of ρ_{tr} at any temperature. We show even more explicitly this effect in Fig.9 where we report the percent variation of the transition density respect to the symmetric case, at various temperatures, for a system having a proton fraction $Z/A = 0.35$.

6   Finite size effects in a Nucleation Mechanism

From the previous simulations it appears that in the few $AGeV$ range, where the approach presented here is valid, we can just enter the mixed phase, since the interacting system will always be rather close to the lower transition density. It is then interesting to discuss the nucleation mechanism for cluster formation, dominant in the metastable regions of a first order phase transition. Thus, in this Section we discuss how the formation of mixed phase is influenced by finite size effects, due to a non-vanishing surface tension at the interface between hadronic (H) and quark (Q) matter. These effects have been investigated in the literature both at zero and at finite temperature [47,48,49]. The crucial quantity to be studied is the work needed to create a bubble of quark matter of radius R, which reads:

$$W_{\min} = [F^Q(P_Q) + P_Q V_Q + 4\pi\sigma R^2 + \frac{16\pi^2}{15}(\rho_V^Q - \rho_C^H)^2 R^5]$$
$$- [F^H(P_H) + P_H V_H], \tag{23}$$

where F is the free energy. The third term in the first bracket describes the energy contribution of a non-vanishing surface tension σ, while the fourth term is related to the Coulomb energy of the drop. The minimal work can be rewritten as

$$W_{\min} = -\frac{4\pi}{3} R^3 [(P_Q - P_H) - \rho_B^Q (\mu_B^Q - \mu_B^H) - \rho_C^Q (\mu_C^Q - \mu_C^H)]$$
$$+ 4\pi\sigma R^2 \frac{16\pi^2}{15} (\rho_C^Q - \rho_C^H)^2 R^5, \tag{24}$$

where both the baryonic (B) and the electric charge (C) appear, since in the here discussed system they are independent [50]. In Fig.10 we show the dependence of $W_{\min}$ on the radius of the drop of quark matter, for two different values of the baryonic chemical potential of the hadronic phase, in the case $P_Q = P_H$.

There are three questions which need to be addressed in order to describe the process of formation of bubbles of quark matter in heavy-ion scattering experiments: the probability of forming a critical bubble on a time-scale compatible with the transient times discussed in Sec.IV, and finally the stability and size of the bubble.

Drop formation rate

The first question concerns the formation time-scale of drops of quark matter. The existence of the non-vanishing surface tension produces a barrier (having a maximum at a radius $R = R_c$) which needs to be overcome. At low temperatures the barrier is bypassed via semi-classical tunneling. At higher temperatures, the ones in which we are particularly interested in this paper, thermal nucleation is the relevant process. The thermal nucleation rate can be estimated as [48]

$$\mathcal{R}_n = \mu_B^4 \exp(-W_c/T), \tag{25}$$

where μ_B is the baryon chemical potential and $W_c = W_{min}(R_c)$ represents the work needed to form the smallest bubble capable of growing. It can be estimated from Eq.(24) neglecting the differences in the chemical potentials. It corresponds to the maximum of the free energy of the bubble of quark matter, which is obtained for a radius $R = R_c$. Here the prefactor has been related to the chemical potential, while, when thermal nucleation is investigated at very large values of the temperature, it is the temperature which drives the prefactor. There is a certain ambiguity on the precise dependence of the prefactor on the chemical potential and/or the temperature. This ambiguity reflects on the precise estimate of the nucleation rate, which is anyway dominated by the exponential factor. We have also explored the possibility of a prefactor $\sim T^4$, obtaining for the critical densities values larger by roughly 10%. The probability of forming a quark bubble inside the hot and dense matter produced by

high-energy scattering of two heavy ions is given by

$$\mathcal{P} = \mathcal{R}_n \, V_0 \, t_0 \ , \tag{26}$$

where t_0 is the duration of the thermal equilibrium of the central region, having a volume V_0, in which large temperatures and densities are reached. The results of the numerical simulations shown in the previous Section indicate a duration $t_0 \sim 10$ fm/c and a volume V_0 of a few ten fm^3. The probability $\mathcal{P}$ of forming a critical bubble has not be too small, if the mixed phase can be produced in a significant fraction of scattering events. We will request that $\mathcal{P}$ is of order unity.

Drop stability

Once a bubble having a radius larger than the critical one is formed, its stability depends on the value of its energy at equilibrium. As it can be seen from Fig. 10, when the chemical potential is not large enough a local minimum (a_2) does develop at a finite value of R. Therefore, the formed drop is metastable, it decays in a finite time and no stable mixed phase can exist. Actually, for small densities and large values of Z/A the local minimum does not exist at all, due to the large contribution associated with repulsive Coulomb energy. For values of the density larger than a critical one, an absolute minimum exists (a_1) and a stable mixed phase can develop. The consequences of the formation of stable droplets have been discussed in the literature in relation with the value of the critical densities in beta-stable matter, in connection with the structure of neutron stars [47]. In that case it is assumed that matter has the possibility to reach complete chemical and mechanical equilibrium, because the system is investigated at an asymptotically large timescale. Therefore, the structures (drops, ropes and slabs) which appear in the mixed phase need to be absolutely stable. The outcome of that analysis is that the critical density, taking into account the absolute stability of the mixed phase, is larger than the critical density estimated neglecting finite size effects. In the present paper, on the other hand, we are not interested in the absolute stability of the mixed phase, but in the possibility of forming drops of quark matter that, although metastable, have a life-time long enough to be observed in high-energy heavy-ion collisions. The crucial time-scale to which the drops life-time has to be compared is the duration t_0 of the thermal equilibrium of the central region in which large temperatures and densities are reached during the scattering process. The numerical results are nevertheless indicating that the density at which the drop becomes absolutely stable is close to the density at which the drop is metastable, but with a long enough life-time. For simplicity, in the following we will therefore consider only stable drops, what corresponds to a small overestimate of the critical density.
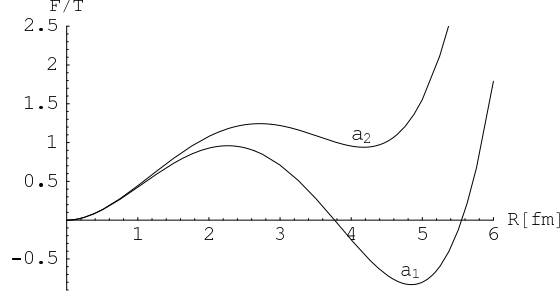
Fig. 10. Free energy as a function of the radius of the drop. Here Z/A = 0.35, T = 50 MeV, B$^{1/4}$ = 160 MeV. The upper (lower) line corresponds to a chemical potential $\mu_B = 1.075$ GeV (1.069 GeV).
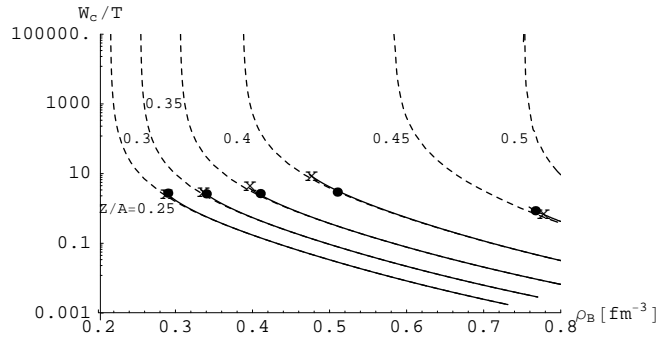

Fig. 11. Work needed to create a drop of quark matter, as a function of the density, for various values of Z/A. Here $T = 50$ MeV, B$^{1/4}$ = 160 MeV. The solid (dashed) lines include (exclude) the Coulomb energy contribution. See text.

Drop size

The final constraint on the minimal density at which the bubble can be generated comes from the volume of the critical bubble, which certainly has not to exceed V_0. Actually its size should be significantly smaller than the size of the central scattering region and, therefore, the radius of the critical bubble has not to exceed 1.5–2 fm^3.

Finite size and finite duration corrections to ρ_{cr}

The actual value of the minimal density at which mixed phase can be formed and observed in heavy ion scattering will be determined by the most restrictive constraint among the ones previously discussed.

In Figs. 11 and 12 we show the work needed to create a critical size drop at a

23

temperature T=50 MeV, as a function of the density and for various values of Z/A. The value of the surface tension has been taken to be $\sigma = 10 \; MeV/fm^2$, as suggested by microscopic calculations [51] and as adopted in other works [52,53,54]. Finally, the value of the bag pressure is $B^{1/4} = 160 \; MeV$ (Fig.11) and $B^{1/4} = 170 \; MeV$ (Fig.12). As it can be seen, W_c strongly depends on Z/A and also on the density, in a way rather similar to the one discussed in Ref.[53] where the nucleation was due to semiclassical tunneling. The solid lines are computed using the complete free-energy of Eq.(24), while the dashed lines are obtained neglecting the Coulomb term. It is interesting to notice that, when the Coulomb energy is neglected, the work W_c diverges at a density ρ_{Gibbs} which corresponds to the critical (transition) density in the absence of surface tension (i.e. the density shown in the previous sections), because at ρ_{Gibbs} the gain in bulk energy vanishes. On the other hand, when the Coulomb term is taken into account, no local minimum does develop below a density $\rho_{metastab}$ (corresponding to the end of the solid lines), which is numerically larger than ρ_{Gibbs}.

As previously discussed, we require the nucleation probability $\mathcal{P}$ to be at least of order unity, what fixes the maximal value of the work to be $W_c/T \sim 10$. In Figs. 11 and 12 we also indicate with a black dot the minimal density ρ_{size}, for each value of Z/A, at which the critical radius $R_c \lesssim 1.8 \; fm$. Finally, small crosses indicate the density ρ_{stab} at which the local minimum of the free energy becomes a global minimum and therefore the drops are absolutely stable.
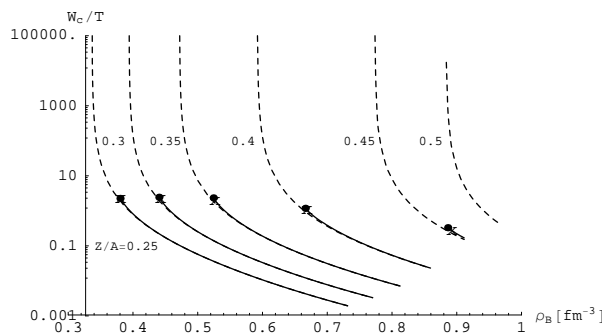

Fig. 12. Same as in Fig.11. Here $B^{1/4} = 170 \; MeV$.

As it can be seen, while finite size effects increase the value of the critical density, the various constraints related to the formation and stability of a drop of quark matter can be satisfied for densities having a rather similar numerical value. The less stringent constraint appears to be the one on the nucleation rate, which is always satisfied once the constraints on the radius and the stability of the drop are imposed [1].

---

[1] It can be interesting to notice that, for small values of B, if the proton fraction is less than 0.4 the main role is played by the constraint on the maximum radius of
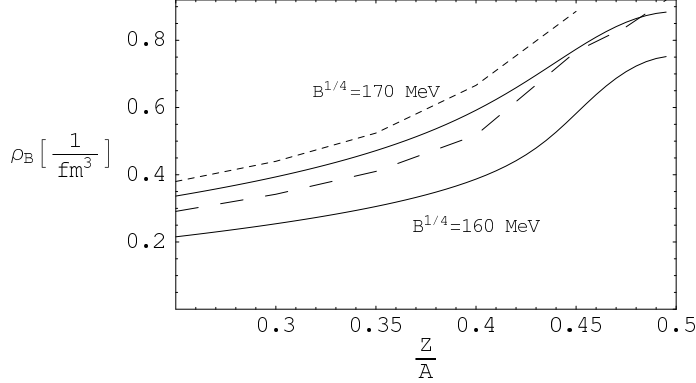
24

Fig. 13. Critical (transition) densities, as a function of Z/A, at $T = 50\ MeV$. The solid lines are obtained neglecting finite-size effects. The long and short-dashed lines take into account these effects and correspond to $B^{1/4} = 160\ MeV$ and to $B^{1/4} = 170\ MeV$, respectively.

In Fig. 13 we show the impact on the critical (transition) densities of finite size effects. Clearly the value of the density at which mixed phase can be observed becomes larger. The increase in the value of the transition density due to finite size effects is larger for smaller values of B. The main result of our work, namely a strong dependence of the transition densities on the value of Z/A, is confirmed by this analysis.

Statistical fluctuations

Before closing this Section, it is worth noticing that statistical fluctuations could help reducing the density at which drops of quark matter form and can be detected. The reason is that a small bubble can be energetically favored if it contains quarks whose Z/A ratio is *smaller* than the average value of the surrounding region. This is again due to the strong Z/A dependence of the free energy, which favors configurations having a small electric charge. If, for instance, we consider a bubble having a volume $\sim 8\ \mathrm{fm}^3$, at the densities here discussed the bubble contains a baryon number of the order of 4. It is clear that, although the average value of Z/A can be significantly larger, random fluctuations can easily produce configurations in which e.g. 4 neutrons are simultaneously present in that small volume. These configurations can easily transform into a bubble of quarks having the same flavor content of the original hadrons, even if the density of the system is not large enough to allow deconfinement in the absence of statistical fluctuations. It is not easy to numerically quantify the relevance of these fluctuations, but we can conclude that, at densities intermediate between the ones corresponding to the neglect

the drop. At variance, for larger values of Z/A the main constraint comes from the existence of the local minimum since the Coulomb energy becomes larger

25

of finite size effects and the ones in which those effects are taken into account, precursory signals of formation of drops of quark matter should appear, if statistical fluctuations are taken into account. Moreover, since statistical fluctuations favor the formation of bubbles having a smaller Z/A, neutron emission from the central collision area should be suppressed, what could give origin to specific signatures of the mechanism described in this paper. This corresponds to a *neutron trapping* effect, supported also by the difference in the symmetry energy in the two phases, which will be discussed in the next section.

7 Deconfinement Precursors

If the transition occurs, we can expect in general a softening of the nuclear EoS, but this can be accounted for even in a pure hadronic picture, i.e. inserting some density dependence in the RMF effective meson couplings. Here we would like to suggest a possible effect which more strictly characterizes the transition model discussed above: a *neutron trapping* (or "neutron distillation") to the quark deconfined clusters. The neutron trapping effect corresponds to the formation of a drop of quarks obtained by deconfining an hadronic drop made mainly by neutrons. The physics behind this isospin migration from the hadron phase to the quark phase is related to the different importance of the symmetry energy, namely, while in the hadron phase we have a large potential repulsion (in particular in the $NL\rho\delta$ case) in the quark phase we only have the much smaller kinetic contribution. In the high density region this effect could be rather relevant: while in a pure hadronic phase neutrons are quickly emitted, when the mixed phase starts forming neutrons are kept in the interacting system up to the subsequent hadronization in the expansion stage.

Let us introduce the *proton fraction* of a quark drop in the mixed-phase as the proton content of the hadron drop from which the quark drop has formed. Clearly, the minimum value of the *proton fraction* is zero, and it corresponds to a drop of quarks produced by the melting of only neutrons. The very low *proton fraction* of the quark clusters formed just at the transition density is reported in the upper panel of Fig.14 for various types of hadronic interaction. In the lower panel of the same figure we report the dependence on the baryon density of the *proton fraction* of the quark clusters in the mixed phase, for a fixed initial isospin content of hadronic matter. Of course, at the upper limit of the mixed phase the initial proton fraction has to be recovered.

Similar results are shown in Tab. 3 where we present the variation of the proton fraction in the quark clusters inside the mixed phase for various initial asymmetries of the hadronic matter. The quantity χ represent the fraction of quark matter. We see a decrease of the transition density with the increase of
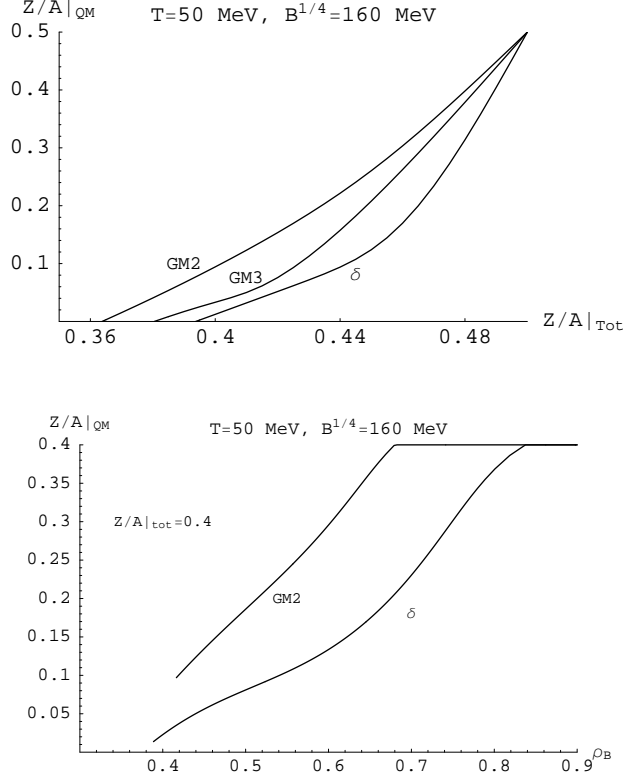
Fig. 14. Isospin migration to the quark clusters. The calculations are performed at a temperature $T = 50\ MeV$ for various hadron effective interactions, as indicated. The MIT bag model without gluon exchange has been used for the quark EoS, with a parameter $B^{1/4} = 160\ MeV$. Upper panel: Proton fraction of the quark phase *at the transition density*. Lower panel: Evolution of the proton fraction of the quark clusters in the mixed phase. Here the initial proton fraction of the hadronic matter is $Z/A = 0.4$.

the initial asymmetry, from $\rho_{tr} = 0.58\ fm^{-3}$ for $Z/A = 0.45$ to $\rho_{tr} = 0.3\ fm^{-3}$ for $Z/A = 0.35$. The calculations are performed at $T = 50\ MeV$ with the $NL\rho\delta$ hadron interaction and with $B^{1/4} = 160\ MeV$.

In conclusion we expect such neutron distillation effect to be particularly efficient if the system is just entering the mixed phase region. Observables related to such neutron "trapping" could be an inversion in the trend of the formation of neutron rich fragments and/or of the π^-/π^+, K^0/K^+ yield ratios for reaction products coming from high density regions, i.e. with large transverse momenta. In general we would expect a modification of the rapidity distribution of the emitted "isospin", with an enhancement at mid-rapidity joint to large event by event fluctuations. A more detailed analysis of these observables is clearly needed and it will be performed in future investigations.

Table 3. Proton Fraction in the Quark Phase.

$\rho(\text{fm}^{-3})$	χ	$Z/A|_q$	$\rho(\text{fm}^{-3})$	χ	$Z/A|_q$
$Z/A = 0.35$			$Z/A = 0.38$		
0.3	0.0	-0.08	0.35	0.0	-0.02
0.38	0.1	0.0	0.37	0.03	0.0
0.54	0.27	0.1	0.54	0.18	0.1
0.68	0.42	0.2	0.68	0.31	0.2
0.77	0.70	0.3	0.76	0.53	0.3
$Z/A = 0.42$			$Z/A = 0.45$		
0.44	0.0	0.05	0.58	0.0	0.12
0.54	0.06	0.1	0.67	0.06	0.2
0.67	0.16	0.2	0.73	0.15	0.3
0.74	0.31	0.3	0.78	0.40	0.4

8   Perspectives

In our work we have investigated the possible formation of a mixed phase of hadrons and quarks during intermediate-energy collisions between neutron-rich heavy ions. In particular we have examined the mechanism of production of a drop of quark matter in the central region, where densities of a few time ρ_0 and temperatures of a few ten MeV can be reached. This is the ideal scenario for testing the formation of a mixed quark-hadron phase, a state somehow similar to the one that could be present in the center of compact stars. An important difference with the compact star scenario is the very low value of strangeness present in the scattering central region. In fact, since weak-decays cannot take place during the short life-time of the high density system, the only possibility of producing strangeness is through associated production but, in the scenario we are discussing, this process has been shown to be very inefficient [33,55]. In the present work we have therefore completely neglected the strangeness production.

The EoS tested in the experiments here discussed shares a rather strict relation with the one to be used *during* the pre-supernova collapse [56]. There, $Z/A \sim 0.34$ [2] and the temperature reached just before the bounce is of the order of a few ten MeV. Moreover, due to neutrino trapping, weak processes are suppressed and typically hyperon production is delayed till the proto-neutron

---

[2] Due to neutrino trapping, the total electron lepton fraction is larger, $Y_{l_e} \sim 0.38$.

star stars deleptonizing. A difference with the heavy-ion scattering scenario is that during the gravitational collapse matter follows an isoentropic EoS, while in our paper we have discussed isothermal EoSs. On the other hand, once a quasi-equilibrium configuration is reached the path previously followed by the thermodynamic variables is irrelevant.

It has been suggested several times that, if a mixed phase forms during the gravitational collapse, this would help Supernovae to explode, due to the softening of the EoS [57,58,59,60,61]. In our paper we have shown that if indeed mixed phase forms during the gravitational collapse, then it is likely that signatures of a mixed phase of hadrons and quarks appear in intermediate-energy scattering between neutron-rich nuclei. The total absence of such signatures would presumably rule out the possibility of deconfinement during the gravitational collapse, although it would definitely not exclude deconfinement at a later stage, when Z/A drops to ~ 0.1 and the central density of the neutron star reaches values of several times ρ_0. Notice anyway that the evidence of the beginning of a phase transition in relativistic heavy ion collisions would have important implications for supernova explosions only if the mixed phase starts appearing at a density of the order of $2\rho_0$, or smaller.

In conclusion, our analysis supports the possibility of observing precursor signals of the phase transition to deconfined quark matter at high baryon density in the collision, central or semi-central, of neutron-rich heavy ions in the energy range of a few GeV per nucleon. A possible signature could be revealed through an earlier softening of the hadronic EoS for large isospin asymmetries, and it would be observed e.g. in the behavior of the collective flows. We also suggest to look at observables particularly sensitive to the expected different isospin content of the two phases, which leads to a neutron trapping in the quark clusters. The isospin structure of hadrons produced at high transverse momentum should be a good indicator of the effect.

References

[1] H.Mueller, Nucl.Phys. **A618**, 349 (1997).

[2] N.K.Glendenning, S.A.Moszkowski, Phys.Rev.Lett. **67**, 2414 (1991).

[3] P.Danielewicz, Nucl.Phys. **A673**, 375 (2000).

[4] P.Danielewicz, R.Lacey and W.G.Lynch, Science **298**, 1592 (2002).

[5] R.Brockmann, R.Machleidt, Phys.Rev. **C42**, 1965 (1990).

[6] T.Gross-Boelting, C.Fuchs, A.Faessler, Nucl.Phys. **A648**, 105 (1999).

[7] B.ter Haar and R.Malfliet, Phys.Rep. **149**, 207 (1987).

[8] T.Gaitanos, C.Fuchs, H.H.Wolter, and A.Faessler, Eur.Phys.J. **A12**, 421 (2001).

[9] V.Greco et al., Phys.Lett. **B562**, 215 (2003).

[10] T.Gaitanos et al., Nucl.Phys. A**732**, 24 (2004).

[11] T.Gaitanos, M.Colonna, M.Di Toro and H.H.Wolter,
Phys.Lett. **B595** , 209 (2004).

[12] B.Liu, V.Greco, V.Baran, M.Colonna, and M.Di Toro,
Phys.Rev. **C65**, 045201 (2002).

[13] A.Chodos et al., Phys.Rev. **D9**, 3471 (1974).

[14] E.Farhi, R.L.Jaffe, Phys.Rev. **D30**, 2379 (1984).

[15] M.C.Birse, Prog.Part.Nucl.Phys. **25**, 1 (1990).

[16] H.J. Pirner, Prog.Part.Nucl.Phys. **29**, 33 (1992).

[17] A.Drago, M.Fiolhais, U.Tambini, Nucl.Phys. **A588**, 801 (1995).

[18] C.Alcock, E.Fahri, A.Olinto, Astrophys.J. **310**, 261 (1986).

[19] P.Haensel, J.L.Zdunik, R.Schaeffer, Astron.Astrophys. **160**, 121 (1986).

[20] A.Drago, A.Lavagno, Phys.Lett. **B511**, 229 (2001).

[21] E.Witten, Phys.Rev. **D30**, 272 (1984).

[22] A.R.Bodmer, Phys.Rev. **D4**, 1601 (1971).

[23] M.Alford, S.Reddy, Phys.Rev. **D67**, 074024 (2003).

[24] A.Drago, A.Lavagno, G.Pagliara, Phys.Rev. **D69**, 057505 (2004). .

[25] X.D.Li et al., Phys.Rev.Lett. **83**, 3776 (1998).

[26] M.Dey et al., Phys.Lett. **B438**, 123 (1998).

[27] A.Pons et al., Astrophys.J. **564**, 981 (2002).

[28] J.J.Drake et al., Astrophys.J. **572**, 996 (2002).

[29] L.D.Landau, L.Lifshitz, *Statistical Physics*, Pergamon Press, Oxford 1969.

[30] N.K.Glendenning, Phys.Rev. **D46**, 1274 (1992).

[31] S.Kubis, M.Kutschera, Phys.Lett. **B399**, 191 (1997).

[32] V.Greco, M.Colonna, M.Di Toro, F.Matera, Phys.Rev. **C67**, 015203 (2003).

[33] G.Ferini, M.Colonna, T.Gaitanos, M.Di Toro, Nucl.Phys. **A762**, 147 (2005).

[34] P.Amore, M.C.Birse, J.A.McGovern, N.R.Walet, Phys.Rev. **D65**, 074005 (2002).

[35] N.K.Glendenning, *Compact Stars*, Springer-Verlag, New York 1997.

[36] T.Neuber, M.Fiolhais, K.Goeke, J.N.Urbano, Nucl.Phys. **A560**, 909 (1993).

[37] J.J.Aubert et al., Phys.Lett. **B123**, 275 (1983).

[38] M.Arneodo, Phys.Rep. **240**, 301 (1994).

[39] R.L.Jaffe, Phys.Rev.Lett. **50**, 228 (1983).

[40] C.E.Carlson, T.J.Havens, Phys.Rev.Lett. **51**, 261 (1983).

[41] S.Barshay, G.Kreyerhoff, Phys.Lett. **B487**, 341 (2000).

[42] K.J.Eskola, V.J.Kolhinen, C.A.Salgado, Eur.Phys.J. **C9**, 61 (1999).

[43] V.Barone, C.Pascaud, F.Zomer, Eur.Phys.J. **C12**, 243 (2000)
Proc. *DIS*2000, Liverpool, World Sci. 2000, p.162.

[44] A.Kayis-Topaksu *et al.* (CHORUS Collab.), Eur.Phys.J. **C30**, 159 (2003).

[45] V.Baran, M.Colonna, V.Greco, M.Di Toro, Phys.Rep. **410**, 335-466 (2005).

[46] E.Santini, T.Gaitanos, M.Colonna, M.Di Toro, Nucl.Phys. **A756**, 468 (2005).

[47] H.Heiselberg, C.J.Petick, E.F.Staubo, Phys.Rev.Lett. **70**, 1355 (1993).

[48] M.L.Olesen and J.Masden, Phys.Rev. **D47**, 2313 (1993) and Phys.Rev. **D49**, 2698 (1994)

[49] M.Kutschera and J.Niemiec, Phys.Rev. **C62**, 025802 (2000).

[50] H.Mueller and B.D.Serot, Phys.Rev. **C52**, 2072 (1995).

[51] M.S.Berger and R.L.Jaffe, Phys.Rev. **C35**, 213 (1987).

[52] D.N.Voskresensky, M.Yasuhira, T.Tatsumi, Nucl.Phys. **A723**, 291 (2003).

[53] Z.Berezhiani, I.Bombaci, A.Drago, F.Frontera, A.Lavagno, Astrophys.J. **586**, 1250 (2003).

[54] A.Drago, A.Lavagno, G.Pagliara, Phys.Rev. **D71**, 103004 (2005).

[55] C.Fuchs, Prog.Part.Nucl.Phys. **56**, 1-103 (2006).

[56] D.Arnett, *Supernovae and Nucleosynthesis*, Princeton Univ. Press, Princeton 1996.

[57] A.B.Migdal, A.I.Cherenoutsan, I.N.Mishustin, Phys.Lett. **B83**, 158 (1979).

[58] M.Takahara and K.Sato, Phys.Lett. **B156**, 17 (1985).

[59] N.A.Gentile *et al.*, Astrophys.J. **414**, 701 (1993).

[60] J.Cooperstein, Nucl.Phys. **A556**, 237 (1993).

[61] A.Drago and U.Tambini, J.Phys. **G25**, 971 (1999).